Science and Technology of Advanced Materials

ISSN: 1468-6996 (Print) 1878-5514 (Online) Journal homepage: www.tandfonline.com/journals/tsta20

Are MXenes viable as conductive, transparent films for industrial applications?

Tiezhu Guo, Shungui Deng, Rene Schneider, Chuanfang Zhang & Jakob Heier

To cite this article: Tiezhu Guo, Shungui Deng, Rene Schneider, Chuanfang Zhang & Jakob Heier (12 Dec 2025): Are MXenes viable as conductive, transparent films for industrial applications?, Science and Technology of Advanced Materials, DOI: 10.1080/14686996.2025.2597556

To link to this article: https://doi.org/10.1080/14686996.2025.2597556

Publisher: Taylor & Francis & The Author(s). Published by National Institute for Materials Science in partnership with Taylor & Francis Group.

Journal: *Science and Technology of Advanced Materials*

DOI: 10.1080/14686996.2025.2597556

Are MXenes viable as conductive, transparent films for industrial applications?

Tiezhu Guo[1,2], Shungui Deng[2], Rene Schneider[2], Chuanfang Zhang[2*] and Jakob Heier [2*]

1 Functional Nanomaterials, Catalonia Institute for Energy Research (IREC), Sant Adrià de Besòs, 08930 Barcelona, Spain

2 Laboratory for Functional Polymers, Empa, Swiss Federal Laboratories for Materials Science and Technology, Uberlandstrasse 129, CH-8600, Dübendorf, Switzerland

[*]Corresponding author ruoshuang123@gmail.com and Jakob.heier@empa.ch

Abstract

Two-dimensional transition metal carbides and nitrides, so-called MXenes, hold significant promise as flexible transparent conductive electrodes (TCEs) in diverse applications. However, MXenes fall below the minimum requirements for industrial use, largely due to factors such as the quality of MXene flakes, electrical conductivity, optical conductivity, and transparent electrode fabrication techniques. In this study, we analyze the relationships among nanosheet size, DC- and optical conductivity and its ratio (σ_{DC}/σ_{op}), and sheet resistance (R_s) of MXene TCEs based on data from published literature. Compared to $Ti_3C_2T_x$ TCEs fabricated with low-quality, small-sized flakes (< 1 μm, σ_{DC}/σ_{op} < 10), those made with high-quality, large-sized nanosheets (>6 μm) with narrow size distributions (σ_{DC}/σ_{op} > 20) exhibit dramatically reduced R_s by several orders of magnitude while maintaining high transmittance. Nevertheless, the σ_{DC}/σ_{op} of continuous $Ti_3C_2T_x$ metallic TCEs saturates at ~24, fairly below the basic requirements for commercial TCEs. By integrating a metallic silver grid onto $Ti_3C_2T_x$ TCEs, a remarkable σ_{DC}/σ_{op} ratio of 330 has achieved, bringing MXene TCEs closer to fulfilling industrial application standards and inspiring greater confidence in their future adoption. Beyond the field of TCEs, the insights gained here could inspire advancements in other areas, such as optoelectronic devices, flexible displays, and energy-efficient transparent technologies. This work provides a framework for the design and development of next-

generation transparent conductive materials with broad implications across various scientific and industrial domains.

Keywords: transparent conductive electrodes, MXenes, figure of merit, percolation, theoretical limitation

Introduction

Transparent conductive electrodes (TCEs) with high conductivity and transparency are essential for a wide range of applications, including transparent supercapacitors, antennas, electromagnetic shielding, and sensors, among others [1]. Traditionally, indium tin oxide (ITO) and fluorine-doped tin oxide (FTO) have served as the first generation of commercial TCEs, offering low sheet resistance (R_s, <10 Ω sq^{-1}) and high transparency (T, >90%) in the visible range [1-4]. However, as ceramic materials, ITO and FTO are prone to cracking and fracturing under relatively low strains of 2~3% [5]. The expansion of microcracks further results in a sharp increase in resistance. This limitation has driven the development of flexible transparent electrodes as replacements for ITO in flexible electronics.

Promising alternatives for flexible TCEs include transparent conductive films based on materials such as silver nanowires, carbon nanotubes (CNTs), PEDOT, graphene, and MXene, but also meshes fabricated from metals [3, 4, 6, 7]. The performance of TCEs is typically characterized by the relationship between transparency (T) and sheet resistance (R_s), as described by the following equation:[8]

$$T=\left(1+\frac{188.5}{R_s}\frac{\sigma_{op}}{\sigma_{DC}}\right)^{-2} \qquad (1)$$

where σ_{op} is optical conductivity, σ_{DC} is DC conductivity, σ_{DC}/σ_{op} is defined as the figure of merit (FOM_e), which is commonly used to evaluate the optoelectronic performance of TCEs. A higher FOM_e indicates that films can be thinning down to the highly transparent region without dramatically increasing its resistance. To replace fragile ITO in many applications, the minimum industrial standard must be met, which requires R_s < 100 Ω sq^{-1} at T > 90% in the visible range [1]. This corresponds to a basic requirement of σ_{DC}/σ_{op} > 35, as derived from Equation 1 [1]. However, many cases demand R_s < 10 Ω sq^{-1} at T > 85%, implying that σ_{DC}/σ_{op} > 220 must be achieved [1].

We note that the upper limits of the optoelectronic properties of graphene-based TCEs have been discussed in previous studies, with maximum figure of merit (σ_{DC}/σ_{op}) values saturate at ~0.7 and 11 for liquid-exfoliated and CVD graphene flakes (without doping), respectively [8]. Clearly, these values fall significantly below the minimum industrial standards. MXene, a family of 2D transition metal carbides, nitrides, and carbonitrides, offers excellent conductivity and being highly transparent when the thickness is several nanometers. Moreover, MXene is water-dispersible and can be processed into transparent conductive films at room temperature using methods such as blade coating, slot-die coating, and spin coating [3, 4, 9]. Some $Ti_3C_2T_x$-based TCEs have demonstrated impressive optoelectronic performance, such as a sheet resistance of 222 Ω sq^{-1} with a transmittance of

92% [4]. However, these results remain insufficient to replace ITO or silver nanowires as TCE materials.

We also note that to date, the true metrics for evaluating MXene-based transparent electrodes have yet to be established. For instance, most studies only report the transmittance (T) and sheet resistance (R_s) of the films, which are often inconsistent due to varying film thicknesses. This variability makes direct comparisons between MXene-based films and other TCE materials difficult. At high transmittance ($T > 90\%$), even slight changes in transparency can lead to a sharp increase in R_s, as the reduced thickness compromises conductive pathways within the electrode. Utilizing the figure of merit (FOM_e) to represent the optoelectronic properties relative to other conductive transparent films remains the most straightforward parameter for comparison. Additionally, we recognize the importance of understanding the upper limit of FOM_e in MXene TCEs, as it tells us the maximum achievable value and the potential in practical applications. However, to date, no reports on the theoretical limitation of FOM_e are available for MXene TCEs, to the best of our knowledge.

In this work, we analyze the relationships between MXene nanosheet size, average conductivity, type of MXene (e.g., $Ti_3C_2T_x$, Ti_2CT_x, V_2CT_x, Ti_3CNT_x, etc.), figure of merit, optical conductivity, and sheet resistance in TCEs at high transparency. We identify the general trends and key factors affecting the optoelectronic performance of TCEs (e.g., the relationship between T and R_s), revealing the potential maximum achievable FOM_e fairly below the minimum industrial requirements. As such, we introduce a metallic Ag mesh onto the MXene TCEs, leading to significantly reduced R_s while marginally affecting T. The Ag mesh-MXene TCEs exhibits a record-high FOM_e up to 330, positioning MXene as a strong candidate for use as a flexible transparent electrode in industrial applications.

Experiments

Fabrication of MXene nanosheets:

0.8 g of LiF was added to 10 ml of 9 M HCl and stirred continuously in an oil bath at 35°C for 10 minutes. Then, 0.5 g of Ti_3AlC_2 was gradually added to the above solution. After 24 hours of reaction, the resulting precipitate was washed with deionized water and centrifuged at 1,500 rcf for 5 min until the supernatant became dark green and the pH approached ~6. Next, 100 ml of deionized water was added to the precipitate and manually shaked until the precipitate was completely redispersed. The solution was degased under argon for 10 min, then sonicated continuously in an ice bath for 60 min at 35 kHz. The dispersion was centrifuged at 1,500 rcf for 30 min and the upper suspension was collected to obtain $Ti_3C_2T_x$ nanosheets.

TCE fabrication

The silver meshes were printed through an aerosol jet printer (Optomec Decathlon AJ-5X) with a nozzle of size 100 μm using the Novacentrix JS-ADEV N250 silver nanoparticle ink on top of the MXene film. During the printing process the ink flow was kept constant, so that the variation of the printing speed (6, 9 and 12 mm/s) controls the printed line width and height, respectively. The uniform $Ti_3C_2T_x$ films were coated onto glass substrate using the slot-die coating method, with the fabrication process and characterization details of the MXene nanosheets provided in our previous study [3]. After drying the ink at room temperature, the samples were annealed at 200°C on a hot plate under argon atmosphere for 2 hours.

Film Characterization

The topography of the printed meshes was obtained by confocal microscopy. The microscope (Leica DCM8) was equipped with a EPI-150X-L objective from Leica, which offers a resolution of 140 nm and 2 nm in x,y- and z-direction, respectively. The sheet resistance (R_s) of the Ag/MXene films was measured using a four-wire measurement method (Keithley 2400 SourceMeter) under ambient conditions. For the MXene films, measurements were conducted using a Jandel RM3-AR four-point probe, with the final value calculated as the average from 10 independent locations on sample. Optical transmittance spectra were recorded using a UV-vis spectrophotometer (Varian Cary 50) over the wavelength range of 350-800 nm. The transmittance at 550 nm, a commonly used reference wavelength for evaluating the transparency of thin films, was determined as the average of five measurements taken from randomly selected positions on each TCE sample. In this study, the FOM_e of the Ag/MXene composites was obtained by fitting the datapoints to Equation 1.

Discussion

Reported Data for Sheet Resistance and Transmittance

The reported data for the T and R_s of MXene-based TCEs show a significant variation, ranging from high-conductivity to high-resistance films, especially in the high transparency (T > 80%) region. We conduct a comprehensive analysis of over 20 studies on MXene-based TCEs, including $Ti_3C_2T_x$, Ti_2CT_x, Ti_3CNT_x, focusing on R_s and T [2-4, 9, 10-19]. Data are extracted from these studies and plotted to show T as a function of R_s, as depicted in **Figure 1**. The results reveal that R_s varies by 2~3 orders of magnitude, from approximately 400 Ω sq^{-1} to around 40 KΩ sq^{-1}, even within similar transparency ranges. This underscores the need to investigate the differences among various MXene-based TCEs and identify the key factors that limit their optoelectronic performance.

Calculated Conductivity Ratio for Published Data

We plotted the figure of merit (FOM_e) values and MXene flake sizes from the same data set. For each system, we generally extract the average or highest value, as shown in **Figure 2a**. It is evident

that there is a clear correlation between the FOM_e of these TCEs and the flake sizes, larger MXene flakes exhibit superior optoelectronic properties compared to those of smaller ones. We define flake size of ~1 μm as the cutoff standard; flakes (several hundred nanometers) smaller than this are typically produced through sonication. Interestingly, the graph can be divided into two sections, MXene films with flake sizes below 1 μm never show σ_{DC}/σ_{op} values larger than 10, while the FOM_e value for MXene films with flake sizes larger than 1 μm tend to exceed 10 with ease. For instance, a maximum FOM_e of ~24 was achieved in $Ti_3C_2T_x$ TCEs with flake size of ~7 μm. Among various types of MXene with similar flake sizes, $Ti_3C_2T_x$ exhibits the highest FOM_e compared to other MXene types, indicating that this type of MXene is the choice of option (**Figure 2b**) [9, 13, 17, 20, 21]. Therefore, $Ti_3C_2T_x$ is selected as the representative material for further analysis of the optoelectronic properties of TCEs. We performed polynomial fitting (other fitting methods yielding more unrealistic results) for the relationship between $Ti_3C_2T_x$ flake sizes and FOM_e (**Figure 2c**), as well as for the sizes of various types of MXenes and FOM_e (**Figure 2d**). The coefficients of determination (R^2) were 0.76 and 0.65, respectively. Although the R^2 values are not particularly high, the fitted curves still capture the trends in the experimental data, and the model parameters are consistent with practical relevance. This suggests that increasing flake size appears to be an effective and feasible approach, particularly for undoped pure MXene.

We further analyze whether variations in σ_{DC} or σ_{op} are responsible for the wide range of FOM_e values observed. Only a few reports provide the thickness of the TCEs, making it impossible to calculate σ_{DC} and σ_{op} in many cases. We extract available data and organized it in Figure 3a. The σ_{op} values vary randomly between 275 and 750 S cm^{-1}, with a median value of 564 S cm^{-1}. This variation depends on the intrinsic characteristics of the material and the number of layers per unit volume. The optical conductivity differences of $Ti_3C_2T_x$ TCEs are further analyzed, with σ_{op} values of 520, 675, 750, 275, 680 S cm^{-1} derived from blade coating, slot-die coating, spin coating, and inkjet printing, gravure printing, respectively [2-4, 18, 19]. Guo et al. demonstrated that TCEs fabricated using blade coating or slot-die coating technologies exhibit higher orientation compared to those produced by spin-coating, as observed in surface morphology [3, 4]. We speculate that the variation in σ_{op} is due to morphological differences between the films, such as surface roughness, free volume, and compactness. Although slight differences in σ_{op} between $Ti_3C_2T_x$ and V_2CT_x (481 S cm^{-1})[20] are reported here, we consider this difference to fall within an acceptable fluctuation range due to the limited data available. However, the average DC conductivity (σ_{DC}) of the TCEs varies significantly, ranging from 3,092 to 15,000 S cm^{-1} (Figure 3b). This suggests that the variation in FOM_e is primarily influenced by changes in σ_{DC}.

In MXene TCEs, charge carriers migrate along the direction with the lowest energy barrier within a single flake, then overcome the interflake tunneling barriers to jump onto another flake. Therefore, the total resistance (R_{tot}) of the TCEs consists of in-plane resistance which represents the inherent resistance (R_{inh}) of the MXene flakes, and interflake resistance (R_{int}) which relates to the quantity of interflake junctions in the horizontal direction and intercalants in the vertical direction [22]. Here, the inherent resistance and the residual Li^+ content are mainly determined by the etching and delamination process. Previous studies have shown that the LiF/HCl etching route results in fewer defects on individual flakes compared to HF etching [23], and reducing the residual Li^+ between layers can improve conductivity [24]. In all cases, the delaminated MXene used for TCE preparation was obtained via conventional HF or LiF/HCl etching routes.

Additionally, the significant difference in conductivity of $Ti_3C_2T_x$-based TCEs reflects variations in the number of interflake tunneling barriers. The number of these barriers depends on the flake sizes and the degree of aggregation or delamination. In films prepared from adequately delaminated, large-sized MXene flakes, there are relatively few interflake barriers. In contrast, as the flake sizes decrease, the number of boundaries significantly increases. This explains why the FOM_e of large-sized MXene films appears in the upper region of Figure 2a, while the FOM_e of small-sized films is found in the lower region. Thus, empirically, the FOM_e of TCEs can be expressed as $FOM_e \propto \sigma_{DC}$, or $FOM_e \propto R_{tot}^{-1} = (R_{inh} + R_{int})^{-1}$. Here, $R_{tot} \approx R_{inh}$, when the flake size approaches infinity, meaning that σ_{DC} and FOM_e values become dependent of the inherent conductivity. Consequently, to achieve the highest performance, we should prepare MXenes with few defects such as pinholes or micropores in the in-plane flakes and smooth edges.

Limiting values of σ_{DC}/σ_{op}

The σ_{DC} and σ_{DC}/σ_{op} of TCEs are influenced by MXene types (intrinsic resistance), flake sizes, and the degree of delamination (interflake resistance). We anticipate that σ_{DC} can be maximized by fabricating large-sized, highly delaminated MXene flakes. In our previous work, we prepared predominantly large-sized $Ti_3C_2T_x$ flakes (12.2 μm) with a narrow size distribution [4]. Films from these flakes exhibit the highest FOM_e of 29, with R_s=77 Ω sq^{-1} at T=83.4%. The TCE demonstrates a high σ_{DC} of 19,325 S cm^{-1}, which, to our knowledge, is the highest reported value from conventional etching methods (HF or HCl/LiF) for Ti_3AlC_2. Unlike liquid-exfoliated graphene flakes, delaminated MXene flakes are obtained by etching the as-received MAX phase using hydrofluoric (HF) or HCl/HF etching methods, or by in situ HF formation methods (such as LiF/HCl with or without intercalants). These methods pose challenges in obtaining large, delaminated $Ti_3C_2T_x$ flakes (larger than 10 μm) with a broad size distribution due to the inherent limitations of the synthesis

process. Gogotsi et al. have reported $Ti_3C_2T_x$ with an average lateral size of 14 μm and a maximum size up to 40 μm, albeit in small quantities [25]. Notably, to meet the minimum industrial standard of FOM_e >35, maximizing the conductivity of TCEs and minimizing interfacial resistance become critical. Assuming the use of ultralarge $Ti_3C_2T_x$ flakes (up to 40 μm) to fabricate TCEs via the slot-die coating process (with an optical conductivity of 675 S cm^{-1}), applying the formula $FOM_e = \sigma_{DC}/\sigma_{op}$, it can be inferred that the DC conductivity of TCEs needs to exceed 23,625 S cm^{-1}, which is evidently achievable. This inference is supported by two key findings, (1) MXene flakes with an average size of 12.2 μm have already achieved a maximum DC conductivity of approximately 20,000 S cm^{-1} [4], demonstrating the potential of larger flakes in reducing interflake resistance and enhancing conductivity. (2) Zeraati et al. reported achieving a DC conductivity of 24,000 S cm^{-1} using $Ti_3C_2T_x$ flakes with an average size of only 1.8 μm via the evaporated-nitrogen minimally intensive layer delamination (EN-MILD) method [26]. We believe that preparing large-sized $Ti_3C_2T_x$ flakes through the EN-MILD method will significantly reduce interflake resistance, which could lead to enhanced DC conductivity and improved σ_{DC}/σ_{op} values, thus enabling superior performance in TCEs applications.

Surpassing limits through integration with metal mesh

Obviously, the pure MXene TCEs based on continuous metallic films give a practical maximum FOM_e of 24, which falls short of the required standard for advanced optoelectronic devices such as the touch panels. Unless ultralarge MXene nanosheets are prepared using special, complex processes as described above (which typically have low yield), this approach, although theoretically feasible, faces significant challenges in practical implementation. To beat the practical limitations, one should revolutionize the TCE architecture by replacing continuous films with mesh structures to substantially improve T without affecting R_s. As such, advanced TCEs can be fabricated using conventional small MXene nanosheets. This is especially true when the mesh is rationally designed, allowing more light to pass through instead of absorbed by the MXene flakes, leading to much increased T. Unfortunately, creating MXene mesh on substrates inevitably decreases the uniformity of corresponding TCEs. To counter such a negative effect, depositing metal grids onto the uniform MXene film to create a metal grid/MXene structure should result in much lower R_s at much higher T, along with uniform electrical, optical and thermal conductivity. As such, we break the FOM_e limitation of MXene TCEs by fabricating metal grid/MXene hybrid TCEs, making them a promising alternative to fragile ITO in applications.

The Ag grids/$Ti_3C_2T_x$ (Ag/MX) hybrid TCEs were accomplished by digitally controlled aerosol jet printing of Ag ink onto dried $Ti_3C_2T_x$ TCEs. The XRD patterns and size distribution of the $Ti_3C_2T_x$ flakes are shown in **Figures 4a, b, c**, with the flake size being approximately 1 μm. Here,

these uniform $Ti_3C_2T_x$ films were deposited onto a glass substrate using the slot-die coating technique, with the details provided in our previous work [3]. The hybrid TCEs were manufactured with an area of 5 × 5 cm², featuring a line pitch of 1 mm in both vertical and horizontal directions, schematics shown in **Figure 4d**. To control the width and height of the Ag lines, we adjusted the printing speed, resulting in three hybrid TCEs variants with average Ag line dimensions of 26.2/0.839 μm, 15.4/0.497 μm, and 14/0.298 μm for width/height, respectively. These variants are labeled as Ag-1/MX, Ag-2/MX, and Ag-3/MX (**Figures 4e, 4f, 4g**). The Ag-1, Ag-2, and Ag-3 grids demonstrated high transparency of 96.4%, 97.5%, and 97.4%, with corresponding sheet resistances of 3.1, 4.6, and 15.8 Ω sq^{-1}, respectively. When these Ag-1, Ag-2, and Ag-3 grids were deposited onto $Ti_3C_2T_x$ TCEs (T = 89%), the transparency of the hybrid TCEs decreased to 82.1%, 83.5%, and 84.7%, with corresponding sheet resistances of 5.6, 9.2, and 21.9 Ω sq^{-1}, respectively (**Figure 4h**). This indicates that the transmittance of the hybrid TCEs primarily depends on the $Ti_3C_2T_x$ TCE at the same line pitch of the Ag grid. As shown in **Figure 4i**, the FOM_e values for Ag-1/MX, Ag-2/MX, and Ag-3/MX were 100, 220, and 330, respectively, representing a significant improvement compared to pure continuous MXene TCEs. To meet the requirements of industrial applications for TCEs that are made from small-sized MXene nanosheets produced using conventional synthesis methods, without relying on strict processes to produce high-quality large-sized MXene nanosheets (which typically have low yield), depositing Ag or other metal mesh structures onto MXenes for hybrid TCE fabrication is a promising design strategy, which could enable MXenes to replace ITO in the future.

Conclusion

In this work, we analyzed both the potential of MXene-based transparent conductive electrodes (TCEs) for industrial applications and their theoretical limitations of FOM_e, while also developing hybrid Ag-grid/MXene TCEs to overcome these challenges. While pure MXene continuous films show promising conductivity and transparency, their figure of merit (FOM_e) saturates at around 29, which is far below the minimum industrial requirement of 35. The limitations of MXene-based transparent conductive electrodes (TCEs) arise from the inherent properties of MXene flakes, such as their type, size, yield, and challenges in achieving high electrical conductivity and low optical conductivity. These factors lead to insufficient technical specifications and pose challenges for large-scale production. Here, key challenges include the difficulty in obtaining large, defect-free flakes and the inability to achieve the required balance of conductivity and transparency. Hybridizing MXene with metal mesh structures is the future for TCEs, as this strategy significantly improves the FOM_e, providing a scalable solution to meet industrial standards and enabling MXene-based TCEs to replace ITO in practical applications.

Acknowledgements

We acknowledge funding from the SFA-AM project grant for SCALAR by the ETH Board.

Conflict of Interest

The authors declare no conflict of interest.

References

1. Zhang C, Nicolosi V. Graphene and MXene-based transparent conductive electrodes and supercapacitors. Energy Storage Mater. 2019;16:102-125. doi: 10.1016/j.ensm.2018.05.003.

2. Zhang C, Anasori B, Seral-Ascaso A, et al. Transparent, Flexible, and Conductive 2D Titanium Carbide (MXene) Films with High Volumetric Capacitance. Adv. Mater. 2017;29(36):1702678. doi: 10.1002/adma.201702678.

3. Guo T, Zhou D, Gao M, et al. Large-Area Smooth Conductive Films Enabled by Scalable Slot-Die Coating of Ti3C2Tx MXene Aqueous Inks. Adv. Funct. Mater. 2023;33(15):2213183. doi: 10.1002/adfm.202213183

4. Guo T, Zhou D, Deng S, et al. Rational Design of $Ti_3C_2T_x$ MXene Inks for Conductive, Transparent Films. ACS Nano. 2023;17(4):3737-3749. doi: 10.1021/acsnano.2c11180.

5. Li W, Akhter Z, Vaseem M, et al. Optically Transparent and Flexible Radio Frequency Electronics through Printing Technologies. Adv. Mater. Technol. 2022;7(6): 2101277. doi: 10.1002/admt.202101277.

6. Gu Z, Tian Y, Geng H, et al. Highly conductive sandwich-structured CNT/PEDOT:PSS/CNT transparent conductive films for OLED electrodes. Appl. Nanosci. 2019;9(8):1971-1979. doi: 10.1007/s13204-019-01006-4.

7. Chen W, Liu L, Zhang H, et al. Flexible, Transparent, and Conductive $Ti_3C_2T_x$ MXene-Silver Nanowire Films with Smart Acoustic Sensitivity for High-Performance Electromagnetic Interference Shielding. ACS Nano. 2020;14(12):16643-16653. doi: 10.1021/acsnano.0c01635.

8. De S, Coleman J. Are There Fundamental Limitations on the Sheet Resistance and Transmittance of Thin Graphene Films? ACS Nano. 2010;4(5):2713-2720. doi: 10.1021/nn100343f.

9. Dillon A, Ghidiu M, Krick A, et al. Highly Conductive Optical Quality Solution-Processed Films of 2D Titanium Carbide. Adv. Funct. Mater. 2016;26(23):4162-4168. doi: 10.1002/adfm.201600357.

10. Li R, Ma X, Li J, et al. Flexible and high-performance electrochromic devices enabled by self-assembled 2D TiO_2/MXene heterostructures. Nat. Commun. 2021;12(1):1587. doi: 10.1038/s41467-021-21852-7.

11. Salles P, Quain E, Kurra N, et al. Automated Scalpel Patterning of Solution Processed Thin Films for Fabrication of Transparent MXene Microsupercapacitors. Small. 2018;14(44):e1802864. doi: 10.1002/smll.201802864.

12. Hantanasirisakul K, Zhao M, Urbankowski P, et al. Fabrication of $Ti_3C_2T_x$ MXene transparent thin films with tunable optoelectronic properties. Adv. Electron. Mater. 2016;2(6):1600050. https://doi.org/10.1002/aelm.201600050

13. Ying G, Dillon A, Fafarman A, et al. Transparent, conductive solution processed spincast 2D Ti_2CT_x (MXene) films. Mater. Res. Lett. 2017;5(6):391-398. doi: 10.1080/21663831.2017.1296043.

14. Ebrahimi M, Mei C. Optoelectronic properties of $Ti_3C_2T_x$ MXene transparent conductive electrodes: Microwave synthesis of parent MAX phase. Ceram. Int. 2020;46(18):28114-28119. doi: 10.1016/j.ceramint.2020.07.307.

15. Mariano M, Mashtalir O, Antonio F, et al. Solution-processed titanium carbide MXene films examined as highly transparent conductors. Nanoscale. 2016;8(36):16371-16378. doi: 10.1039/c6nr03682a.

16. Salles P, Pinto D, Hantanasirisakul K, et al. Electrochromic Effect in Titanium Carbide MXene Thin Films Produced by Dip-Coating. Adv. Funct. Mater. 2019;29(17):1809223. doi: 10.1002/adfm.201809223.

17. Hantanasirisakul K, Alhabeb M, Lipatov A, et al. Effects of Synthesis and Processing on Optoelectronic Properties of Titanium Carbonitride MXene. Chem. Mater. 2019;31(8):2941-2951. doi: 10.1021/acs.chemmater.9b00401.

18. Wen D, Wang X, Liu L, et al. Inkjet Printing Transparent and Conductive MXene ($Ti_3C_2T_x$) Films: A Strategy for Flexible Energy Storage Devices. ACS Appl. Mater. Inter. 2021;13(15):17766-17780. doi: 10.1021/acsami.1c00724.

19. Abdolhosseinzadeh S, Schneider R, Jafarpour M, et al. MXene Inks for High-Throughput Printing of Electronics. Adv. Electron. Mater. 2025;11(2):2400170. doi: 10.1002/aelm.202400170.

20. Ying G, Kota S, Dillon A, et al. Conductive transparent V_2CT_x (MXene) films. Flatchem. 2018;8:25-30. doi: 10.1016/j.flatc.2018.03.001.

21. Valurouthu G, Maleski K, Kurra N, et al. Tunable electrochromic behavior of titanium-based MXenes. Nanoscale. 2020;12(26):14204-14212. https://doi.org/10.1039/d0nr02673e

22. Tang J, Wan H, Chang L, et al. Tunable Infrared Sensing Properties of MXenes Enabled by Intercalants. Adv. Opt. Mater. 2022;10(17):2200623. doi: 10.1002/adom.202200623.

23. Alhabeb M, Maleski K, Anasori B, et al. Guidelines for Synthesis and Processing of Two-Dimensional Titanium Carbide ($Ti_3C_2T_x$ MXene). Chem. Mater. 2017;29(18):7633-7644. doi: 10.1021/acs.chemmater.7b02847.

24. Lee J, Wyatt B, Davis G, et al. Covalent Surface Modification of $Ti_3C_2T_x$ MXene with Chemically Active Polymeric Ligands Producing Highly Conductive and Ordered Microstructure Films. ACS Nano. 2021;15(12):19600-19612. doi: 10.1021/acsnano.1c06670.

25. Shekhirev M, Busa J, Shuck C, et al. Ultralarge Flakes of $Ti_3C_2T_x$ MXene via Soft Delamination. ACS Nano. 2022;16(9):13695-13703. doi: 10.1021/acsnano.2c04506.

26. Zeraati A, Mirkhani S, Sun P, et al.. Improved synthesis of $Ti_3C_2T_x$ MXenes resulting in exceptional electrical conductivity, high synthesis yield, and enhanced capacitance. Nanoscale. 2021;13(6):3572-3580. doi: 10.1039/d0nr06671k.

Figures

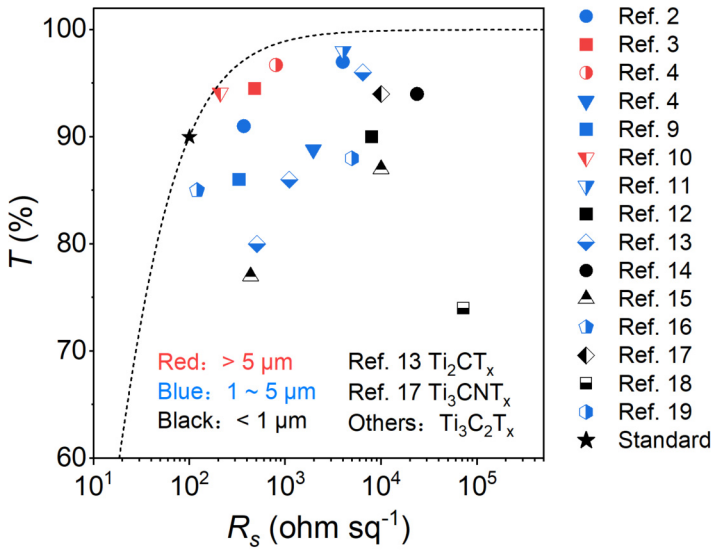

Figure 1. Transmittance (T) and sheet resistance (R_s) data from literature reports [2-4, 9-19]. Data are divided into 3 categories (MXene flake sizes of < 1μm, 1-5 μm, > 5 μm). The black star is the lowest industrial standard value for transparent electrodes.

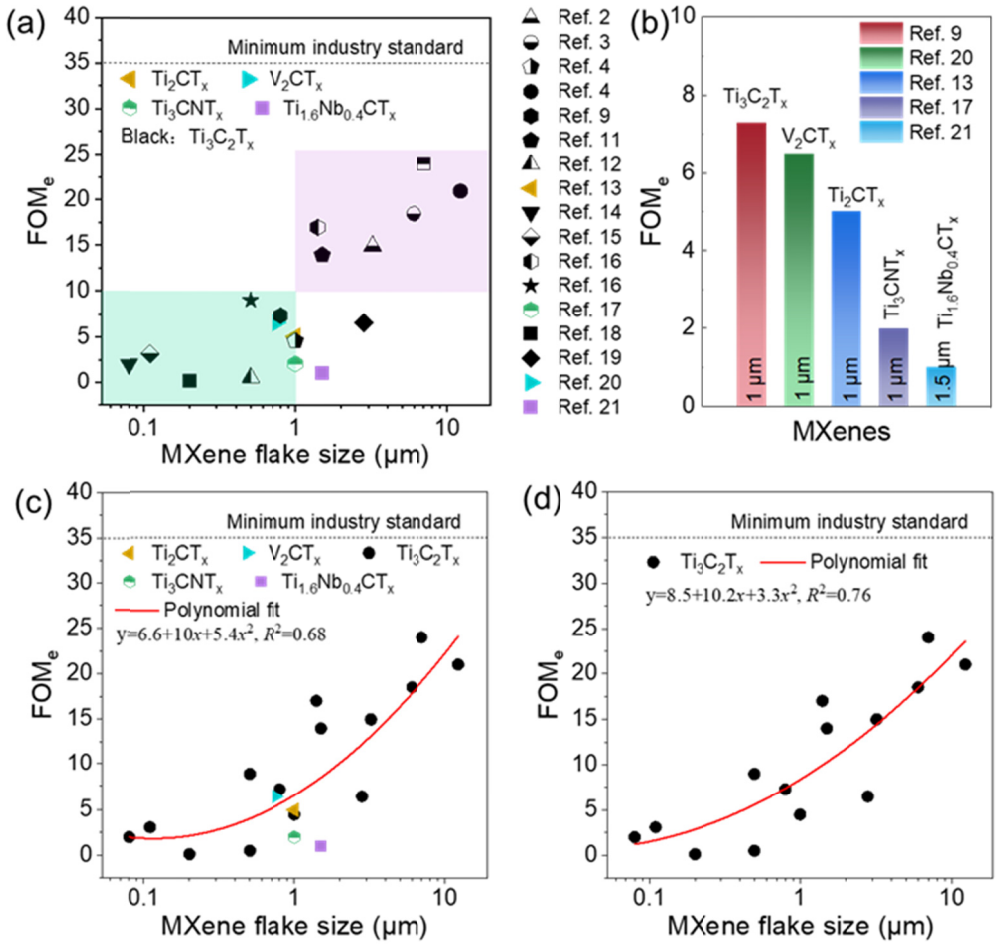

Figure 2. (a) FOM_e values of various MXenes as a function of flake sizes. The FOM_e (σ_{DC}/σ_{op}) values are extracted or fitted from T and R_s data reported in the literature. (b) Comparison of figure of merit (FOM_e) of different-type MXene at similar flake sizes. (c) Fitting curve of FOM_e value and flake sizes from $Ti_3C_2T_x$ dataset. (d) Fitting curve of FOM_e value and flake sizes from various MXene datasets.

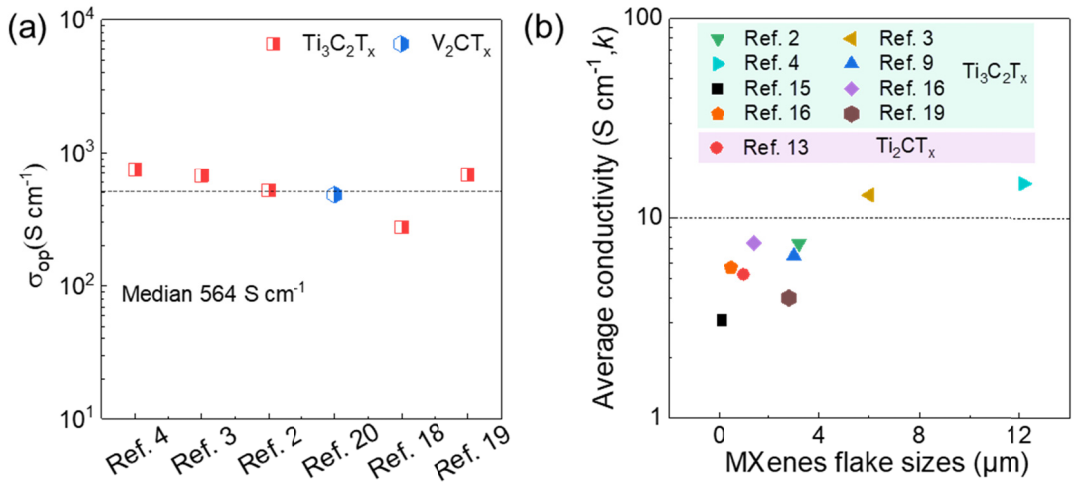

Figure 3. The optical conductivity (a) and DC conductivity (b) extracted from the literature.

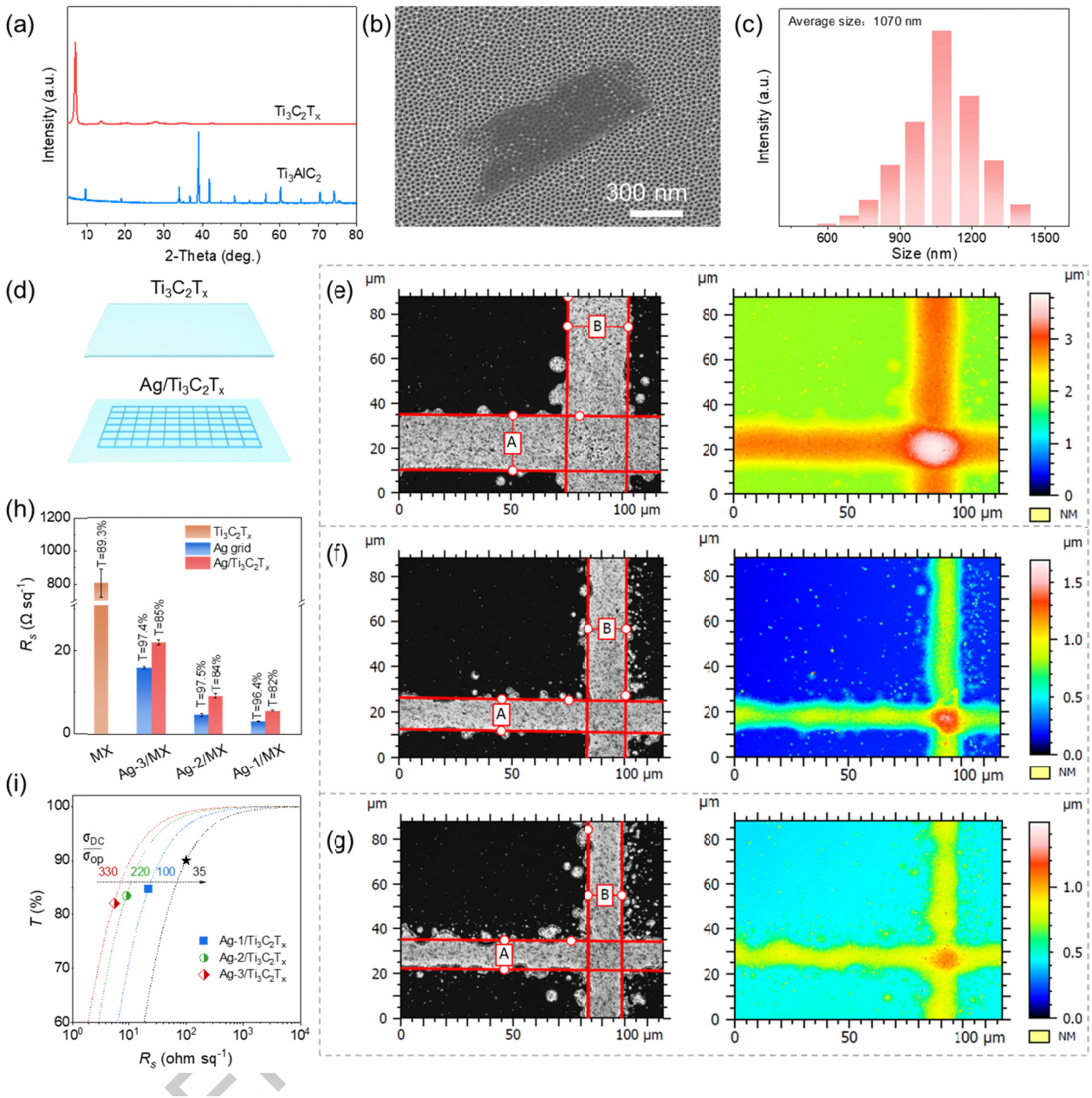

Figure 4. (a, b, c) XRD patterns, SEM image, and particle size distribution of the $Ti_3C_2T_x$ flakes, respectively. (d) Scheme of the printed grids on the MXene TCE. (e, f, g) The width and height of Ag lines under printing speed 6, 9, 12 mm s^{-1}, respectively. Left side: width, Right side: height. (h) Sheet resistance and transmittance of $Ti_3C_2T_x$, Ag grid and Ag-grid/MX hybrid TCEs. $Ti_3C_2T_x$ flakes size is about 1 μm. Ag grid was printed onto the $Ti_3C_2T_x$ TCE. (i) The relationship of Ag-grid/MX hybrid TCEs between T with R_s, also included are fitting curves according to Equation 1. The black star is the lowest industrial standard value for transparent electrodes.

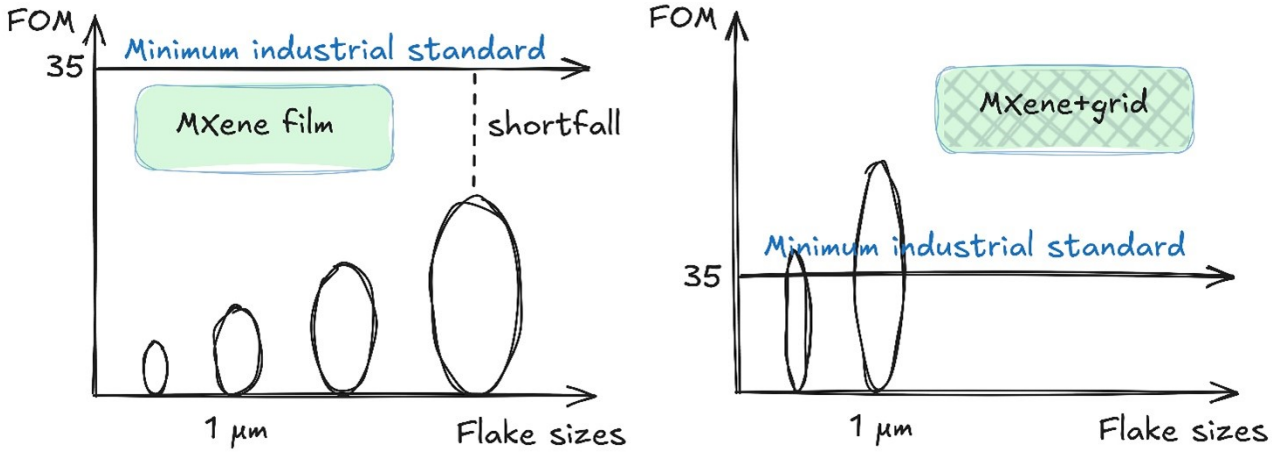

GraphicalAbstract1

Impact Statement

A coated MXene film alone cannot meet industrial standards for transparent conductive electrodes; however, when integrated with a printed silver grid, it successfully achieves the required transparency and conductivity levels.